Applied Catalysis B: Environmental 89 (2009) 49–57

Contents lists available at ScienceDirect

Applied Catalysis B: Environmental

journal homepage: www.elsevier.com/locate/apcatb

Electrochemical investigation of a propane-fed solid oxide fuel cell based on a composite Ni–perovskite anode catalyst

Massimiliano Lo Faro [a,*], Daniela La Rosa [a], Isabella Nicotera [b], Vincenzo Antonucci [a], Antonino Salvatore Aricò [a]

[a] CNR-ITAE Institute, Via Salita S. Lucia sopra Contesse 5, IT-98126 Messina, Italy
[b] Università degli Studi della Calabria, IT-87036 Arcavacata di Rende (CS), Italy

ARTICLE INFO

Article history:
Received 17 July 2008
Received in revised form 7 November 2008
Accepted 14 November 2008
Available online 24 November 2008

Keywords:
Propane
Direct oxidation
La_2NiO_4
Gadolinia-doped ceria
IT-SOFC

ABSTRACT

A composite Ni–perovskite anode was investigated for operation in dry propane-fed intermediate temperature solid oxide fuel cells (IT-SOFC). A $La_{0.6}Sr_{0.4}Fe_{0.8}Co_{0.2}O_3$ (LSFCO) perovskite, characterized by mixed electronic–ionic conductivity, was used to support a highly dispersed Ni-phase. However, the catalyst structure was modified during SOFC operation. X-ray diffraction analysis of the electrocatalyst showed that, after operation, Ni was mainly present as La_2NiO_4; whereas, the LSFCO structure was partially modified into a lanthanum-depleted $SrFe_{1-x}Co_xO_{3-y}$ (SFCO) perovskite structure. These results were corroborated by X-ray photoelectron spectroscopy (XPS). Transmission electron microscopy (TEM) analysis showed the presence of a suitable dispersion of a nanosized Ni-phase and a strong interaction of Ni-enriched particles with the perovskite substrate. High reaction rates for the propane reaction were achieved with this electrocatalyst while minimizing carbon deposition. Power densities of about 300 mW cm^{-2} for dry propane oxidation were obtained at 800 °C in the presence of a thick gadolinia-doped ceria electrolyte. Fuel cell time-tests indicated promising electrochemical stability.

1. Introduction

The use of dry hydrocarbons in intermediate temperature (500–800 °C) solid oxide fuel cells (IT-SOFCs) has been intensively investigated in the recent years [1–3]. A significant attention has been focused on methane electro-oxidation by using different electrocatalysts including Cu/CeO_2, Ni–Cu and various perovskites [1–5]. The perovskite materials have shown promising performances for natural gas combustion [5,6] and suitable activity for oxygen reduction [7] showing bi-functional properties. Encouraging results have been achieved at temperatures below 800 °C, especially in the presence of ceria electrolyte [1,4,5].

Some attempts have been addressed to the oxidation of larger molecular weight hydrocarbons in SOFCs [1,8]. It has been observed that the reaction rate for the oxidation of propane is lower compared to methane, especially because it involves several steps and formation of intermediates [8–15]; moreover, oxidation of dry propane is more affected than methane by the cracking process producing carbon fibers that poison the anode surface. This occurs especially in the case of Ni–cermet catalysts. These cermets usually contain up to 65 vol.% of metallic Ni, as electronic conducting phase, and yttria-stabilised zirconia as ion conducting phase [16,17]. Such composite catalytic layer allows an extension of the triple-phase boundary where the electrochemical reaction occurs. The formation of carbon deposits occurs under both direct oxidation and steam reforming conditions at intermediate temperatures in the presence of low steam to carbon (S/C) ratios [18,19]. However, an excess of water injected into the stream reduces the process efficiency and increases the water-management constraints.

Propane is the main component of liquefied petroleum gas (LPG). This is an interesting fuel for SOFCs. It is cheap, widely available and it can be liquefied to facilitate its storage for specific applications. Due to these properties, desulphurised LPG has good properties to be used as fuel in portable power sources. For such applications, the oxidation of dry propane in SOFC is favoured since it does not require any special fuel or water management, thus, reducing the complexity of the system. For portable applications, the main requirements concern with the obtainment of suitable power densities and the simplicity of design as well as operation at intermediate temperatures. In this regard, ceria-based electrolytes have good perspectives since the lower electrical efficiency, usually associated to a partial electronic conductivity of this material as compared to the conventional yttria-stabilised zirconia, is compensated by the higher conductivity at lower temperatures.

* Corresponding author. Tel.: +39 090 624241; fax: +39 090 624247.
E-mail address: lofaro@itae.cnr.it (M. Lo Faro).

0926-3373/$ – see front matter © 2008 Elsevier B.V. All rights reserved.
doi:10.1016/j.apcatb.2008.11.019

Recently, several investigations have been addressed to the use of Ru as promoter of propane oxidation in IT-SOFCs [8,20–23]. Yet, the high cost of Ru suggests searching for an alternative catalyst formulation with similar activity at intermediate temperatures. Ni-doped perovskite catalysts have been studied for the oxidation of hydrocarbons in SOFCs [24]. The attention has been concentrated on the $La_{0.8}Sr_{0.2}Cr_{0.8}Mn_{0.2}O_{3-\delta}$ (LSCM) perovskite that showed suitable chemical stability at high temperature under reducing conditions but poor electrochemical characteristics at intermediate temperatures [3,24]. In this work, we have investigated the electrochemical behaviour of a composite anode composed of Ni, LSFCO and gadolinia-doped ceria ($Ce_{0.8}Gd_{0.2}O_{1.9}$) electrolyte. The LSFCO perovskite has suitable perspectives for intermediate temperature operation since it is characterized by proper electronic and ionic conductivity under such conditions [1,2,5,6,9]. This material is normally used in SOFCs as cathode due to the fact that it is less stable in a reducing environment giving rise to the formation of metallic Fe and Co species that could promote carbon deposition. In the CGO electrolyte-based SOFCs, the significant oxygen availability at the anode/electrolyte interface may compensate for this effect [5]. Such oxygen availability is due to the occurrence of the following processes. O^{2-} ions flow from the cathode due to the fuel cell electrical process; O_2 molecules are pumped from the cathode into the anode compartment (oxygen pump effect) due to the different oxygen partial pressure between the cathode and anode separated by the anionic ceramic membrane. An additional oxygen flow towards the anode is promoted by reduction of ceria-based electrolytes at the anode and reoxidation at the cathode. This process occurs even under open circuit voltage (OCV) conditions. It is exemplified below in the case of hydrogen as reducing agent:

$$2Ce^{4+} + H_2 + O^{2-} \rightarrow 2Ce^{3+} + H_2O(\text{anode}) \quad (1)$$

$$2Ce^{3+} + 0.5O_2 \rightarrow O^{2-} + 2Ce^{4+}(\text{cathode}) \quad (2)$$

The Ce^{3+} ions formed at the anode are transferred to the cathode. This occurs by an electron hopping mechanism from Ce^{3+} to Ce^{4+} ions in the electrolyte. The Ce^{3+} ions are thus oxidized at the cathode by the oxygen molecules. The result is a net electron flow from the anode to the cathode that determines the partial electronic conductivity of ceria-based electrolytes. This is electrically balanced by the O^{2-} ions flow to the anode.

An interaction between the dispersed Ni-phase and the perovskite at high temperature modifies the chemical and electronic properties of the materials and, thus, the propensity of nickel to form carbon deposits. In this catalytic layer, Ni is not present in the bulk form as in a classical cermet, but, it is highly dispersed on the perovskite support. Accordingly, the electronic conducting properties are exerted by the support; whereas, Ni acts as promoter for the catalytic activity. Furthermore, this strong interaction between Ni and perovskite may favour the formation of an oxidized Ni-phase that could be stable under mild reducing conditions.

From a thermodynamic point of view, the direct oxidation process should be favoured since the Gibbs free energy change compares favourably to the reforming and carbon deposition processes [25]. Yet, due to kinetic and electrochemical constraints including C–C bond cleavage for C_3H_8, unefficient transport of O^{2-} ions through the electrolyte and poor availability of these ions at the interface, the side-reactions may readily occur. The water formed as reaction product in the anodic electrochemical reaction, may promote an internal reforming process especially in the presence of a high fuel utilization or low gas hourly space velocity (GHSV). Formation of H_2 and CO is not deleterious for the process since both molecules electrochemically react with O^{2-} ions to form H_2O and CO_2; whereas, carbon deposition usually deactivates the catalyst. It has been shown in the literature that some Ni catalysts, such as metallic Ni–Cu, Ni–Co, tolerate small amounts of carbon deposition or carbon fibers formation [1,4,9]. These fibers usually improve the electronic conductivity inside the catalytic layer.

The aim of this work is to investigate the oxidation process of dry propane in an IT-SOFC at a Ni-modified perovskite anode catalyst in the presence of ceria-based electrolytes. The catalyst has been investigated in terms of structure, chemistry and morphology. The reaction products at the anode compartment outlet during continuous fuel cell operation have been analyzed and some critical aspects have been discussed.

2. Experimental

2.1. Anode catalyst preparation

The Ni-modified LSFCO catalyst was prepared by the incipient wetness method [20]. The LSFCO powder (Praxair) was impregnated at 50 °C with a solution of Ni nitrate in water. The powder was first dried and then calcined in oven at 500 °C for 2 h (heating rate, 2 °C/min; cooling rate, 2 °C/min). The resulting Ni content was 10% on LSFCO (w/w). Three reduction procedures were investigated. A first reduction was carried out in 5:95 H_2/Ar flow at 400 °C (30 min) preventing the LSFCO modification in this step of catalyst preparation. A second reduction process at 800 °C (30 min) was investigated to study the structural modifications. In a third experiment, the Ni/LSFCO catalyst was calcined at 1100 °C for 2 h and subsequently reduced at 800 °C, in hydrogen for 2 h according to the conditioning procedure of the SOFC cell. For comparison, a 10% Ni–CGO catalyst was prepared by using the same procedure. It was subjected to the same calcination treatment at 1100 °C for 2 h and reduction at 800 °C for 2 h in H_2.

2.2. Physico-chemical characterization of the anode catalyst

Morphology and microanalysis studies of the Ni-modified perovskite catalyst were carried out by a FEI CM12-EDX instrument operating at 120 kV and equipped with LaB_6 filament. The sample was dispersed in ethanol in an ultrasonic bath; a few drops of this solution were deposited on a copper grid. The morphology of the anode layer after operation was investigated by scanning electron microscope (SEM-EDX, FEI XL30).

XRD analysis was carried out with a X'PERT Philips diffractometer equipped with Cu Kα source. A Bragg–Brentano set-up was used for the powders; whereas, a thin film configuration (grazing angle 0.5°) was used to study the anode layer after operation. X-ray photoelectron spectroscopy (XPS) measurements were performed by using a Physical Electronics (PHI) 5800-01 spectrometer. A monochromatic Al Kα X-ray source was used at a power of 350 W. Spectra were obtained with pass energies of 58.7 eV for elemental analysis (composition) and 11.75 eV for the determination of the chemical species. The pressure in the analysis chamber of the spectrometer was 1×10^{-9} Torr during the measurements. To compensate for surface-charging effects, the calibration of the binding energy (B.E.) scale was made with reference to the B.E. at 284.6 eV of the adventitious carbon. The quantitative evaluation of each element was obtained by dividing the integrated peak area, after Shirley background subtraction, by atomic sensitivity factors, which were calculated from the ionization cross-sections, the mean free electron escape depth and the measured transmission functions of the spectrometer by using the PHI Multipak 6.1 software.

2.3. Manufacturing and testing of the solid oxide fuel cell

The CGO electrolyte powder was compacted by uniaxial pressing (300 MPa). The green pellet was treated at 1450 °C for 6 h in air to obtain a supporting electrolyte membrane ($\rho_{rel} > 95\%$).

The anode powder was fabricated by mixing in a ball milling the Ni-modified perovskite catalyst with gadolinia-doped ceria (CGO). This composite material was deposited onto one face of a CGO electrolyte pellet (250 μm) and fired at 1100 °C for 2 h in air. The thickness of this active catalytic layer was about 15 μm. The synthesis of the CGO powder was made by a co-precipitation method described elsewhere [4]. For the current collector a gold paste was used.

The LSFCO cathode (PRAXAIR) was deposited on CGO by spraying. The deposit was fired at 1100 °C for 2 h in air. The SOFC device used in this study consisted of a button cell (1 cm^2 active area). The cell was mounted on an alumina tube, sealed with quartz adhesive (AREMCO) and initially heated with an He stream at the anode, whereas, the cathode was under static air. During the heating ramp to 800 °C, the gas was switched to H_2 at 400 °C and the cell reached the OCV. The cell was switched from OCV to 500 mV allowing electrochemical current flow (O^{2-} ions) preventing an extensive reduction of perovskite. After conditioning in H_2 at 800 °C for 2 h, the anode was fed with dry propane under working condition at 500 mV cell voltage. Two methodologies were selected for operation in dry propane. In a first time-study, the anode was fed with 100% dry propane with a flow rate corresponding to about 150 times the fuel stoichiometry required by the faradic process with the cell operating at 1 A cm^{-2}. Several redox cycles of the anode were carried out during this time-study. The redox cycle consisted in an interruption of C_3H_8 flow for a few hours. During this short period a small amount of oxygen is generally pumped into the anode compartment promoting burn-off of any carbon deposit formed during operation [4,5,8–12,20]. In a second approach, a fuel stoichiometry as close as possible to the practical operation conditions was selected for the time-study. In this second experiment, propane was diluted with helium (2% C_3H_8 in He). The propane feed was about two times the stoichiometry that required by the cell to operate at 1 A cm^{-2}. Static air was used at the cathode in both cases to simulate passive mode operating conditions. Polarization and AC-impedance experiments were carried out at different times during operation. Electrochemical polarizations and AC-impedance measurements were performed on an electrolyte supported single cells at different temperatures by using an AUTOLAB PGSTAT30 Metrohm potentiostatical frequency–response analyzer equipped with 20 A booster. Gold wires and gold paste were used as current collectors for the cell. A thermocouple was positioned close to the cell. Impedance spectra were obtained in the frequency range from 10 mHz to 1 MHz with applied AC-voltage amplitude of 10 mV rms. All impedance measurements were taken at 500 mV cell voltage.

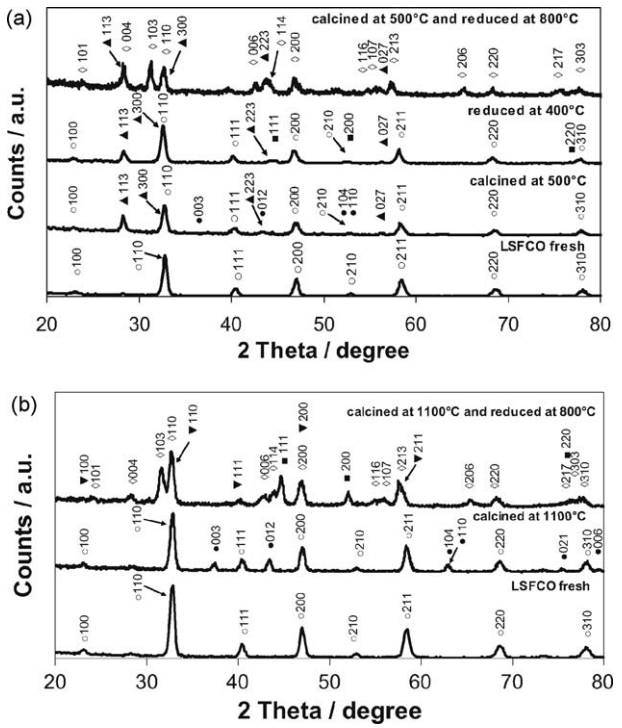

Fig. 1. (a) XRD patterns of the Ni-modified LSFCO catalyst calcined at 500 °C and reduced at 400 °C and 800 °C: (○) LSFCO, (●) NiO, (◄) $Sr_2Fe_{1-x}Co_xO_5$, (◇) La_2NiO_4 and (■) Ni. (b) XRD patterns of the Ni-modified LSFCO catalyst calcined at 1100 °C and reduced in H_2 at 800 °C: (○) LSFCO, (●) NiO, (◄) $Sr(Fe_{0.5}Co_{0.5})O_{2.88}$ [26], (◇) La_2NiO_4 and (■) Ni.

2.4. Analysis of the reaction products from direct propane electro-oxidation

The analyses of the residue fractions from the fuel cell electrochemical process (time-studies) were performed by IR, DSC, gas–mass and NMR techniques: IR spectra were carried out by FTIR Jasco 4200 spectrometer, gas-mass spectrum by Agilent 6890 (detector agilent 5973), ^1H and ^{13}C NMR spectra were recorded on a Bruker AVANCE 500 (11.7 T) spectrometer at room temperature.

3. Results

3.1. Structure and morphology of the anode catalyst

A structural analysis of the anode catalyst was carried out after different ex situ thermal treatments. The treatments were selected on the basis of the anode conditioning and operating procedures of the cell. The first XRD analysis was carried out on the as-prepared Ni-modified LSFCO catalyst, the catalyst calcined at 500 °C and after reduction in hydrogen at 400 °C and at 800 °C. These patterns are shown in Fig. 1a. A small segregation of LSFCO in the form of $Sr_2Fe_{1-x}Co_xO_5$ (JCPDS 40-0874) is already envisaged upon calcination at 500 °C (Fig. 1a). Less evident are the reflections of NiO (JCPDS 22-1189) in the sample calcined at 500 °C (Fig. 1a), possibly due to the small particle size. After the ex situ reduction in hydrogen at 400 °C, the peaks of metallic Ni (JCPDS 4-850) become evident without significant variation of the perovskite structure (Fig. 1a). After reduction at 800 °C, the metallic Ni is less evident and a new phase assigned to La_2NiO_4 (JCPDS 33-712) appears (Fig. 1a). The $Sr_2Fe_{1-x}Co_xO_5$ phase is also detected after reduction at 800 °C (Fig. 1a) but less evident.

The sample thermal treated in air at 1100 °C for 2 h shows essentially the peaks of NiO and LSFCO phases (Fig. 1b). It appears that the perovskite structure is not altered by this treatment. The $Sr_2Fe_{1-x}Co_xO_5$ phase previously detected in a small amount after calcination at 500 °C is not observed upon calcination at 1100 °C (Fig. 1b). After reduction at 800 °C in H_2 of the sample previously fired in air at 1100 °C, the formation of La_2NiO_4 is clearly observed together with metallic Ni. Both perovskite and the new formed La_2NiO_4 are the major phases after this treatment. Possibly, the high temperature firing process carried out before the reduction treatment stabilises the perovskite structure. This structure is now somewhat depleted of La and, thus, enriched in Sr with respect to the raw sample. This is evidenced by a slight shift of the perovskite diffraction peaks to smaller Bragg angles. A close matching of the new perovskite phase reflections with $Sr(Fe_{0.5}Co_{0.5})O_{2.88}$ [26] corroborates such evidence. The La_2NiO_4 phase occurs as a

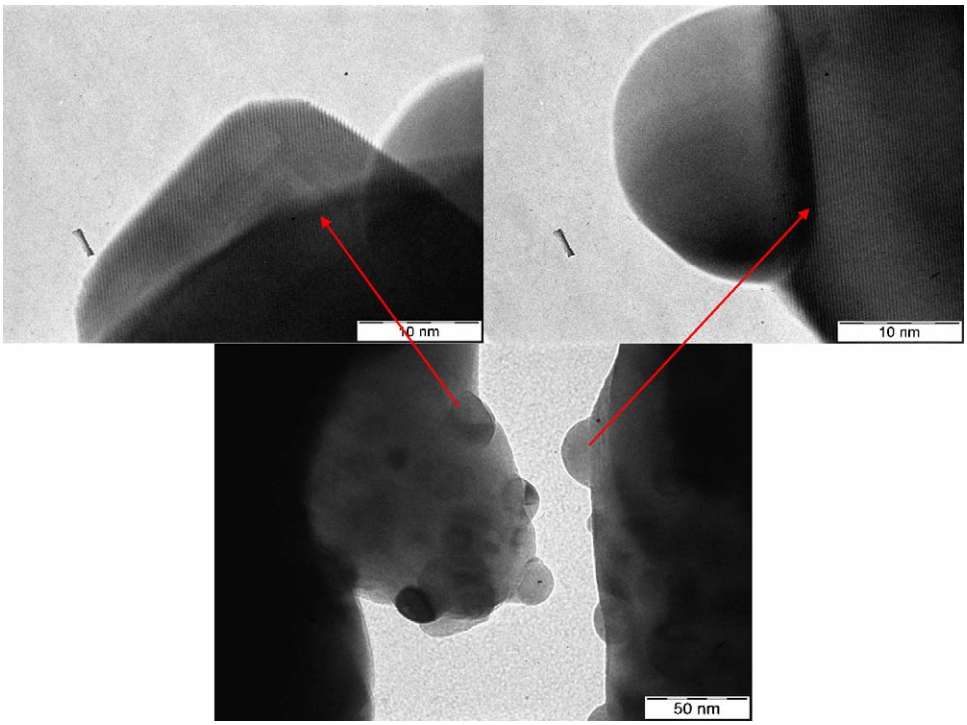

Fig. 2. TEM micrographs of the Ni-modified LSFCO catalyst treated at 1100 °C in air and subsequently reduced in H_2 at 800 °C.

consequence of the interaction of the perovskite with NiO at high temperature.

Fig. 2 shows the transmission electron micrographs of the anode catalyst after thermal treatment in air at 1100 °C and subsequent reduction at 800 °C. The nickel containing particles are well dispersed on the perovskite support. They have dimension of about 30 nm and show spherical or squared shape. The particles with squared shape show lattice distances close to those of La_2NiO_4 (JCPDS 33-712); whereas, the lattice distances in the support are similar to those of the strontium enriched perovskite structure [26] and the LSFCO phase. This analysis was carried out after a reduction of 2 h in H_2 that corresponds to the SOFC conditioning time in this environment at 800 °C. The spherical particles show a strong interaction with the support. The presence of similar lattice distances at the interface between the particles and the support may be an indication of lanthanum reaction with Ni oxide to form a new oxidized phase. The La_2NiO_4 is usually avoided in SOFC anodes because of its insulating characteristics. However, in the present anode, these nanosized particles essentially play a catalytic role; whereas, the electronic conductivity is assured by the large particles of the perovskite support and especially by the gold paste conductor. TEM analysis clearly shows that the Ni-phase does not form a continuous network as opposite of the electron conducting perovskite support. An energy dispersive X-ray analysis (EDX) was carried out during TEM measurements by focusing the electron beam either on the bulk of a Ni-modified perovskite catalyst agglomerate or on the surface of this sample (Fig. 3). Due to the large size of the beam spot and measurements conditions, it was difficult to get rid of the X-ray scattering of the Cu-grid and support during the analysis of the particles deposited on the perovskite surface. However, an enrichment of Ni and La as well as a depletion of Sr on the catalyst surface is envisaged (Fig. 3).

3.2. Investigation on surface electronic states

The surface chemistry of the anodic catalyst (thermal treatment at 1100 °C for 2 h and reduction at 800 °C for 2 h in H_2) was investigated by XPS (Fig. 4). The La 3d (Fig. 4a) spectra show the presence of two doublets for both Ni-modified LSFCO catalyst and LSFCO support. These are associated to the presence of lanthanum in an oxidized state [27]. The profile of the XP-doublet in the B.E. region from 840 eV to 830 eV (La $3d_{5/2}$), where no interference of nickel occurs, is different in the two samples. This is probably due to a different structural arrangement of La species with the same oxidation state. The high B.E. region of the La 3d (La $3d_{3/2}$) spectrum is affected by the interference of Ni $2p_{3/2}$ signal (Fig. 4b). This makes complicate an univocal identification of the Ni oxidation state based on the B.E. shift. Two small satellite peaks at B.E. of about 862 eV and 880 eV associated to Ni $2p_{3/2}$ (854 eV) and Ni $2p_{1/2}$ (872 eV), respectively, were identified. These usually occur in the Ni (2+) oxidized phase and they are associated to the behaviour of oxidized Ni species [27]. In the present case, the strong interference of La $3d_{3/2}$ doublet does not allow a clear identification of the metallic Ni (852.7 eV) [27]; yet, its presence on the surface is not discarded. The occurrence of metallic Ni in the

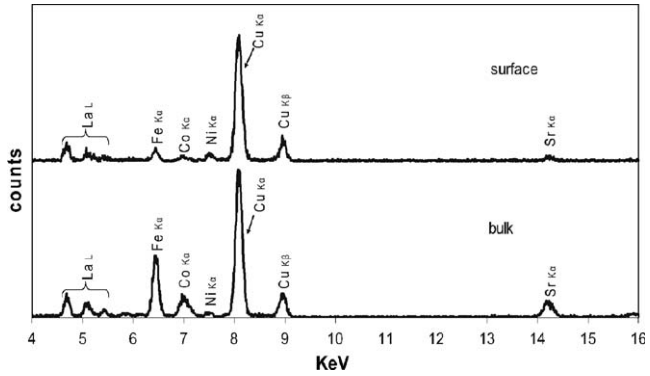

Fig. 3. EDX analysis during TEM measurements for the bulk and surface of the Ni-modified LSFCO catalyst after calcination at 1100 °C (2 h) and reduction at 800 °C in hydrogen (2 h). The Cu signal is from the grid. Fe Kβ (not shown) partially overlaps with the Co Kα peak.

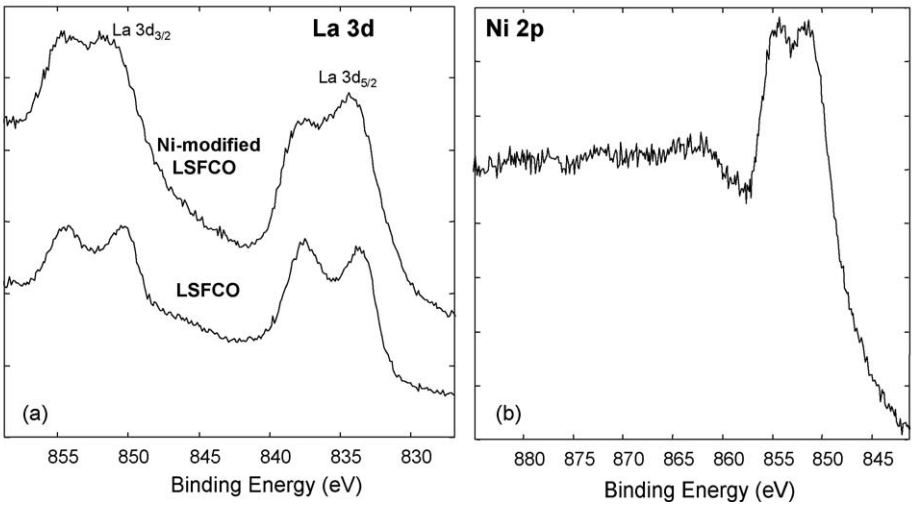

Fig. 4. XPS analysis of the raw LSFCO support and Ni-modified LSFCO catalyst treated at 1100 °C and reduced at 800 °C: (a) La 3d spectra and (b) Ni 2p spectrum.

bulk was already observed by XRD after reduction at 800 °C in H_2 for 2 h (Fig. 1b).

3.3. Electrochemical analysis with high fuel flow rate

AC-impedance analysis of the SOFC cell operating with H_2 in the temperature range 700–800 °C at a cell voltage of 0.5 V, is shown in Fig. 5. The polarization resistance (R_p) is obtained from the low frequency (R_{LF}) intercept on the real axis subtracted by the high frequency (R_{HF}) intercept ($R_p = R_{LF} - R_{HF}$). The SOFC shows an appropriate polarization resistance decreasing from about 0.54 Ω cm^2 to 0.1 Ω cm^2 as the temperature increases from 700 °C to 800 °C. The series resistance (R_s) derived from the high frequency intercept on the real axis of the Nyquist plot, decreases from 0.43 Ω cm^2 at 700 °C to 0.25 Ω cm^2 at 800 °C (Fig. 5). These ohmic losses are mainly due to the thick 250 μm supporting membrane electrolyte.

Polarization curves carried out in H_2 (Fig. 6) show that the maximum power density increases with temperature (421 mW cm^{-2} at 800 °C); whereas, the OCV decreases due to a small electronic conduction in the CGO electrolyte [28]. The mixed electronic–ionic conduction of CGO electrolyte does not allow the cell to reach high OCV values associated with a very low oxygen partial pressure at the anode.

The electrochemical experiments carried out in dry propane and reported in Figs. 7–9 concern the use of a high flow rate of pure propane (150 times the stoichiometric flow at 1 A cm^{-2}). Impedance spectra were carried out at 800 °C after different operation times of the cell in the presence of dry propane (high flow rate), at 0.5 V cell voltage. Fig. 7 shows that the initial series resistance in propane is slightly larger than in H_2 (0.41 Ω cm^2 vs. 0.25 Ω cm^2). During operation, the increasing depth of the reduction process and possibly a small amount of carbon deposition on the catalyst causes the decrease of both ohmic and polarization resistances [29].

For what concerns the ohmic resistance, results similar to those obtained in hydrogen, were obtained in propane after 101 h of operation, i.e. R_s = 0.28 Ω cm^2 at 800 °C (Fig. 7). The observed R_p values in propane at 800 °C (about 0.55 Ω cm^2 at 0 h and 0.33 Ω cm^2 after 101 h), indicate suitable reaction rates (Fig. 7).

Fig. 8a shows the polarization curves in dry propane (high fuel flow rate) at 800 °C after different operation times of the cell for the Ni-modified perovskite catalyst. A maximum power density of about 300 mW cm^{-2} was obtained after 101 h of lifetime. The output power density of the present device 300 mW cm^{-2} at 800 °C is quite promising if we consider that it is mainly affected by ohmic drop and low OCV. These are essentially related to the electrolyte membrane thickness (250 μm) and a small electronic conduction of the electrolyte, respectively.

In order to evaluate the influence of the gold current collector on the anode performance, a SOFC cell equipped with an Au/CGO anode was investigated. The achieved performance was one order

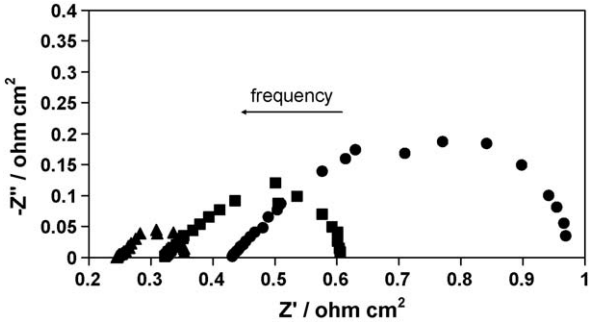

Fig. 5. AC-impedance spectra for the SOFC cell operating at 500 mV in the presence of H_2 at different temperatures: (●) 700 °C, (■) 750 °C and (▲) 800 °C.

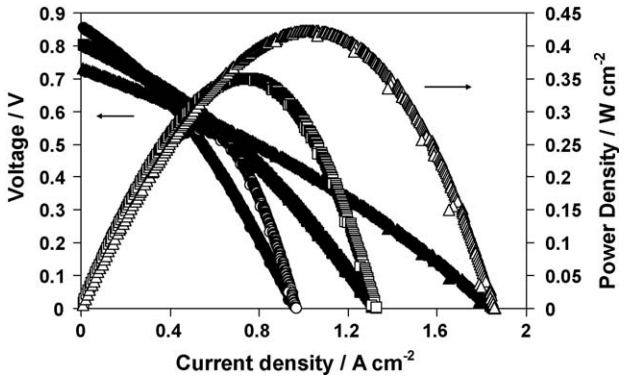

Fig. 6. Polarization curves at different temperatures in the presence of H_2 feed at the anode and static air at the cathode: (●) 700 °C, (■) 750 °C and (▲) 800 °C.

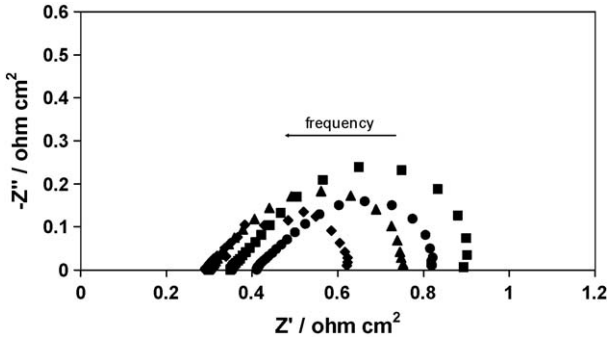

Fig. 7. AC-impedance spectra at 800 °C for the SOFC cell at 500 mV operating in the presence of dry C_3H_8 and static air at different operational times: (●) 0 h, (■) 5 h, (▲) 23 h and (◆) 101 h.

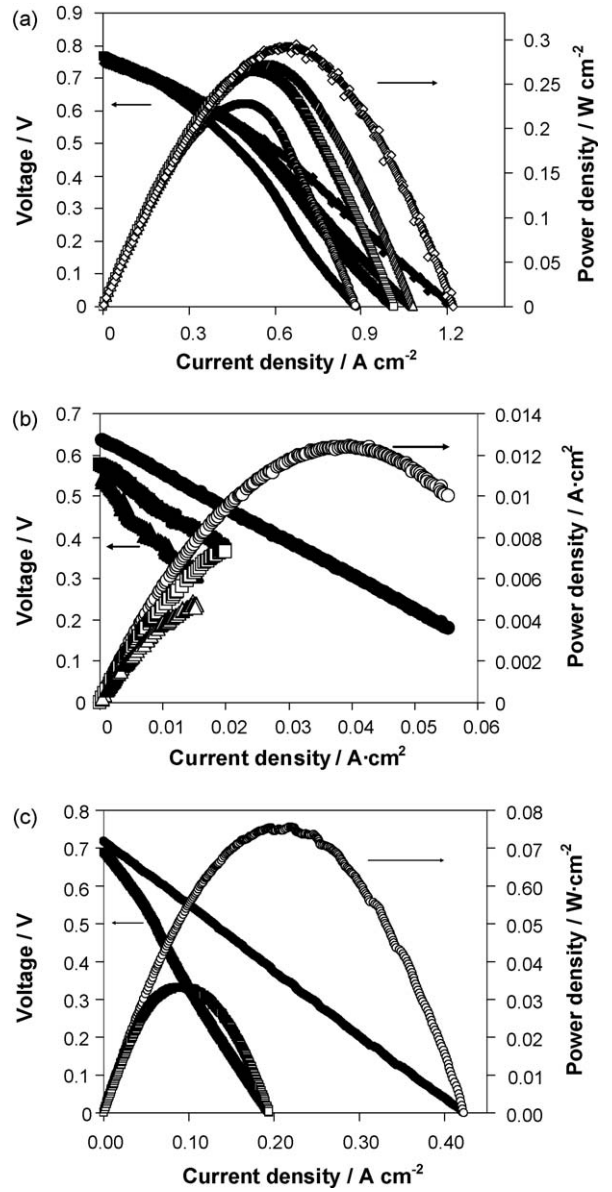

Fig. 8. (a) Polarization curves at different operating times in dry C_3H_8 for the Ni-modified catalyst and static air at 800 °C: (●) 0 h, (■) 5 h, (▲) 23 h and (◆) 101 h. (b) Polarization curves at different operating times in dry C_3H_8 for the pure gold current collector catalyst layer and static air at 800 °C: (●) 0 h, (■) 72 h and (▲) 95 h. (c) Polarization curves at different operating times in dry C_3H_8 for a Ni–CGO catalyst layer and static air at 800 °C (●) 5 h and (■) 20 h.

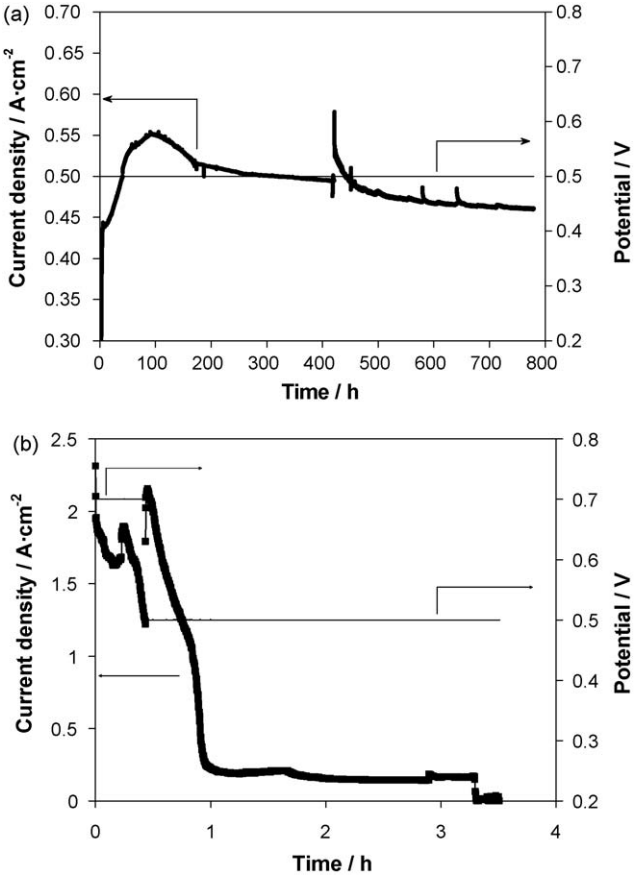

Fig. 9. (a) Time-test for the Ni/LSFCO catalyst in the presence of a large flow rate of C_3H_8 at 800 °C. (b) Time-test for the raw perovskite support only in the presence of a large flow rate of C_3H_8 at 800 °C.

of magnitude lower than that recorded in the presence of the Ni–perovskite catalyst with progressive decrease of OCV with the operation time (Fig. 8b). This confirms that the Au/CGO combination is almost inert towards both reforming and oxidation of propane. The low OCV reflects a poor catalytic activity that further decrease with the operating time.

Similarly, a Ni/CGO catalyst with 10 wt%. Ni content as in the Ni-modified perovskite sample was investigated for comparison (Fig. 8c). The best performance of 75 mW cm^{-2} was achieved after 5 h of operation in dry propane. Subsequently, it decreased with time (Fig. 8c). These results clearly indicate that the anodic process is activated by the presence of the Ni–perovskite catalyst in the presence of CGO electrolyte.

A time-study is shown in Fig. 9a for the Ni–perovskite anode-based cell operating in dry propane. A high flow rate of pure propane as in the above experiments was used (see Section 2). For comparison, a short time-test under same conditions is reported for the LSFCO perovskite support only (Fig. 9b). A fast deactivation of the perovskite support was observed after few hours (Fig. 9b). The Ni-modified perovskite catalyst showed initially low current density; but, a rapid increase of performance was recorded during the first hours of operation. The cell performance increased for the Ni-modified LSFCO catalyst in the first 101 h; after that a maximum performance was achieved; subsequently, the cell potential decreased progressively. Such behaviour was attributed to an initial improvement of conductivity within the anode layer due to a small carbon deposition; whereas, when an excess of deposited carbon impeded the reactant to reach some of the catalytic sites, the performance decreased [29]. Several short redox

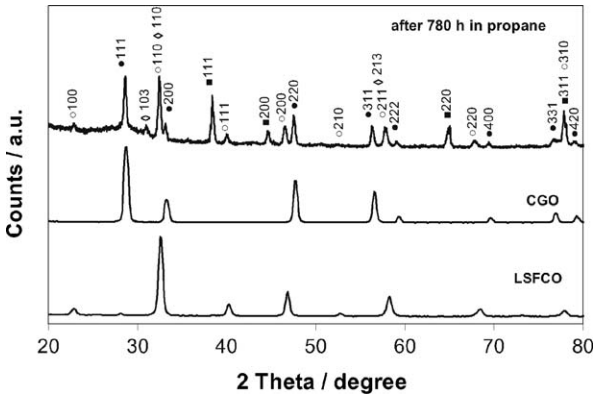

Fig. 10. Comparison between the anode catalyst before and after about 780 h operation at 800 °C with a high propane flow rate. The XRD patterns after 780 h also include the typical pattern of the CGO electrolyte: (◇) La_2NiO_4, (●) CGO, (○) LSFCO and (■) Au.

cycles were carried out, e.g. after about 410, 580, 645 h operation, with duration of 6, 2 and 3 h, respectively. These produced only a temporary increase of current density, possibly due to the burn-off of carbon deposits (Fig. 9a). After this time-test, the process was shut-down by feeding hydrogen to the anode up to reach room temperature and the cell was subsequently dismantled.

The anode was analyzed firstly by grazing-angle XRD (Fig. 10). This technique, generally used to study thin films, resulted appropriate to investigate the anode layer while minimizing the strong X-ray scattering from the bulk electrolyte. The XRD analysis of the cell after shut-down showed that the catalyst structure was modified during operation. Despite, the reducing conditions at the anode, no metallic Ni, Fe and Co were observed. Ni was mainly present as La_2NiO_4. Gold and CGO are present in the pattern because an Au paste was used as current collector and CGO as electrolyte. The peaks of a La-depleted perovskite phase are also evident. It appeared from XRD that no significant amount of carbon fibers were present on the anode after cell shut-down. This aspect may be explained with the availability of oxygen species at the anode/electrolyte interface and the presence of a thin (15 μm) anode active layer. However, a small amount of tar deposits is not discarded (see Supporting information). SEM observation (Fig. 11) of the anode layer after prolonged operation showed that a few carbon fibers or tar deposits were effectively formed on the surface. These may be responsible for the improved electronic

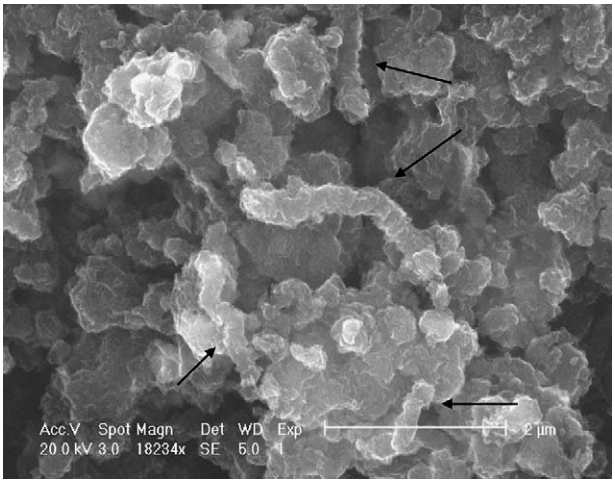

Fig. 11. SEM image of tar or carbon deposits (indicated by arrows) on the anode surface after 780 h operation with dry propane at 800 °C (high flow rate).

conductivity of the cell at the beginning of the duration test, but also responsible for the decay. However, it was considered that the formation of small amounts of carbon deposits did not affect so negatively the SOFC performance in the presence of the dry hydrocarbon, in this accelerated test, as it usually occurs for a classical Ni–cermet (complete catalyst deactivation in a few hours). Probably, this is due to the fact that Ni is well dispersed on the support and the occurrence of La_2NiO_4 in the final catalyst. Furthermore, it is pointed out that the oxide anode catalyst support is more tolerant than Ni–cermets to redox cycles; thus, the excess of carbon deposits may be burned off by transient exposure to small amounts of oxygen. This can be pumped from the cathode through the electrolyte by using the oxygen pump effect.

3.4. Analysis of reaction products

The gaseous reaction products from the anodic process in the tests carried out with a high propane flow rate were monitored by using chromatographic analysis. The liquid was condensed and the remaining water traces removed by using a $Mg(ClO_4)_2$ bed before that gas sampling was carried out by the gas chromatograph (micro-GC). During the time-test, the CO_2 yield was about 70% of that expected from the recorded current density and Faraday law. Smaller amounts of CO (5%) and H_2 (∼10%) were also detected. Usually, these compounds electrochemically react at the catalyst surface. Possibly, the CO and H_2 molecules which were formed in the outer electrode layers where no suitable triple-phase boundary is present are removed from the catalyst surface by the high flow rate before they can electrochemically react. This is a clear indication of the occurrence of an internal reforming process of propane with the water formed in the process. In addition to these gases and water, a small amount of a highly viscous pitchy fluid, coming out from the anode compartment during the accelerated (high flow rate) time-study was detected. This product was not detected during short electrochemical tests; but, it was collected only after prolonged operation. The tarry residue consisted mainly of dioctyl-phthalate (liquid fraction) and polyoxymethylene (solid fraction) as determined by NMR (^1H and ^{13}C), DSC, FT-IR and gas–mass techniques (see Supporting information). It is known that *n*-butane at 800 °C undergoes to free-radical decomposition in the gas phase forming tar deposits [30]. A similar mechanism may also occur for propane. Our experiments carried out in the presence of gold only at the anode showed that the same tar formation occurred after about 100 h operation in dry propane with pure gold anode. Accordingly, the occurrence of tar is possibly not related to the specific Ni–perovskite catalyst used in this study.

3.5. Electrochemical experiments with practical propane feed

To evaluate the behaviour of the catalyst under conditions which are close to the application, an appropriate propane feed was used in a second time-study (Fig. 12). Due to the small cell dimension (1 cm^2), and large scale of mass flow controllers, it was necessary to dilute propane with He (2% C_3H_8 in He) to achieve practical propane feed. A propane feed corresponding to a propane stoichiometry of two, calculated at the current density of 1 A cm^{-2}, was fixed during the experiment. However, the total gas flow rate (propane and helium) was comparable to the previous experiment. Initially, the performance was smaller than that recorded in the previous experiments due to the dilution effect. It rapidly increased with time up to surpass that achieved in the experiment with high stoichiometry. A fluctuation of current density during this experiment was observed. This was probably associated to the high degree of dilution for the fuel. A few redox cycles of about 1–2 h were carried out. These did not affect significantly the

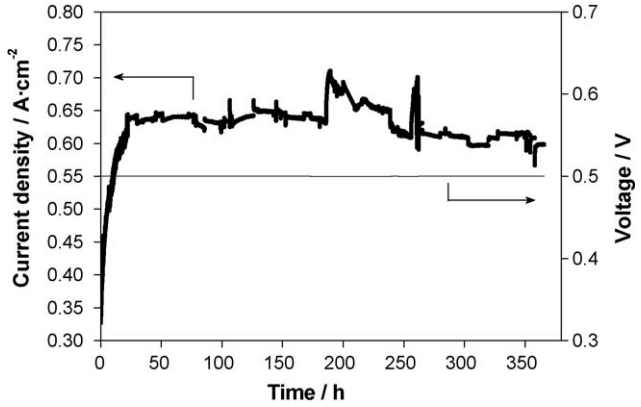

Fig. 12. Time-study of the SOFC cell operating with dry propane and practical flow rate at the anode and static air at the cathode at 800 °C. The flow rate was equal to two times the stoichiometry at 1 A cm^{-2}.

electrochemical behaviour (Fig. 12). A proper performance was achieved during such time-study after about 30 h; the current density remained at a suitable value for more than 300 h. This indicates that carbon deposition did not affect significantly the process as in the previous case. Probably, in the presence of a practical fuel flow rate, the water formed in the process could be more effective in reducing carbon deposition and promoting internal reforming especially in the outer layers of the anode where the triple-phase boundary is less effective. In previous experiments carried out by Kim et al. [31] for butane oxidation, a high flow rate was effective in reducing the amount of carbon deposition by sweeping away the growing tar molecules in the gas phase. In our work, we have diluted propane with helium to maintain the same total gas flow rate in the two experiments with high and small propane feed. Furthermore, it was demonstrated by Kim et al. [31] that in the presence of water (S/C = 1.5) the carbon formation associated to butane decomposition is decreased even not stopped completely. The use of a practical propane feed may increase the actual steam to carbon ratio on the catalyst surface influencing the carbon deposition rate. A power density exceeding 300 mW cm^{-2} was achieved with dry propane after 60 h operation (Fig. 13a). The AC-impedance spectrum (Fig. 13b) shows the presence of two well-defined semicircles. The low frequency intercept is similar to that observed after 101 h in the previous time-study carried out with high propane flow rate. The appearance of the low frequency semicircle may be related to the fuel dilution with helium at the anode. A significant increase of faradic efficiency for CO_2 formation to about 90% was achieved in this second time-study experiment with practical propane feed. CO and H_2 were also observed in these operating conditions, as in the case of pure propane, clearly indicating the occurrence of an internal reforming process promoted by the water formed at the anode surface. The amount of organic products was smaller than that observed in the previous lifetime experiment with high propane flow rate; but, they were still detected after prolonged operation. A further optimisation of the operating conditions is necessary to further depress these side processes.

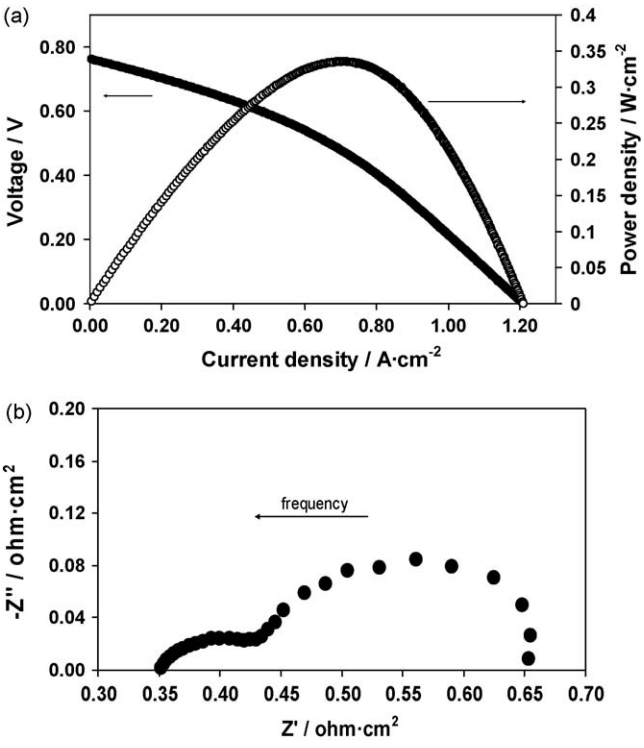

Fig. 13. (a) Polarization curve collected after 60 h in dry propane and static air at 800 °C. (b) AC-impedance spectrum collected after 60 h in dry propane and static air at 800 °C.

4. Discussion

It is envisaged that the performance and CO_2 yield of the present SOFC process may be greatly enhanced if a thin electrolyte is used. A reduced ohmic drop and a larger flow of O^{2-} ions at the interface would be beneficial for the process in terms of performance and CO_2 yield. Furthermore, a high electrical efficiency may be achieved, if the CGO membrane is replaced by another electrolyte characterized by a higher ionic transport number and comparable conductivity at intermediate temperatures [32].

The polarization resistances of the SOFC process with dry propane feed were quite promising indicating that this catalyst can properly operate without the need to use noble metals like Ru, Rh, etc. to promote the oxidation process [8,33]. As well known, Ni promotes the C–H bond scission that is the first step in the oxidation process; but, it also increases significantly the probability of irreversible deposition of carbon species at the surface [34]. This especially occurs when Ni is in the metallic form. In the present case, Ni is mainly in an oxidized phase, i.e. La_2NiO_4; accordingly, this catalyst shows to be less favourable to the carbon deposition process than conventional Ni–cermets. Furthermore, being the La_2NiO_4 phase highly dispersed on a conductive ceramic support (perovskite), there is no significant influence of the poor electronic conduction of La_2NiO_4.

The cleavage of the carbon–hydrogen bond is considered to be the activation step in the overall oxidation process [34], together with the removal of adsorbed species by effect of the O^{2-} ions. The suitable polarization resistances recorded in the present work would indicate that the present La_2NiO_4 catalyst can promote the cleavage of C–H bonds in propane. On the other hand, CGO has been identified as a suitable oxidation catalyst for both H_2 and methane [15,33]. The rate determining step for CGO only as catalyst presently appears to be related with the scission of C–H bond [15]. Thus, the composite catalytic layer forms a bi-functional catalyst. The presence of H_2 and CO in the outlet gas stream indicates the occurrence of an internal reforming with the water formed in the electrochemical process. This step is likely catalysed by the Ni–perovskite catalyst whereas CGO mainly acts as an oxidation catalyst [33]. The analysis of the reaction products in combination to the produced electricity and fuel cell performance shows that the catalyst has suitable characteristics to oxidize small

organic compounds such as propane in the presence of ionic oxygen (O^{2-}); however, further efforts should be addressed to the increase of CO_2 yield in the direct oxidation process.

5. Conclusions

The electro-oxidation of propane at a Ni-modified perovskite catalyst was investigated at intermediate temperatures (800 °C) in a CGO electrolyte supported cell. The SOFC cell showed suitable power density and polarization resistance. Physico-chemical analyses indicated that a chemical modification of the perovskite support occurred in a reducing environment. The formation of a new Ni-phase on the surface and a La-depleted perovskite was observed.

No significant carbon deposits were detected on the catalyst surface after SOFC operation with practical propane flow rate. However, some carbon deposit was observed on the alumina tube and tar was detected in the outlet stream. This is possibly related to the propane decomposition in the gas phase at 800 °C. It appears that the presence of Ni as an oxidized La_2NiO_4 phase finely dispersed on the perovskite support favours C–H bond scission in the hydrocarbon while minimizing the growth of carbon fibers on the catalyst. Furthermore, if the La_2NiO_4 is properly dispersed on an electronic conducting support, no significant ohmic constraints are registered.

The achieved performance for propane oxidation was quite interesting even in the presence of a thick electrolyte membrane. CO_2 yield and electric efficiency need to be further improved (the maximum power density was achieved at about 500 mV); however, they appear promising for portable applications [35]. The fuel utilization in these SOFC devices should be sufficiently high (>90%) for portable applications. The advantage of this process relies on the high energy density of propane/LPG with respect to hydrogen gas; a fuel efficiency of 100% does not appear to be the main pre-requisite for portable systems due to the low fuel consumption in these devices. What is expected from such systems is a high energy density, simplicity of design and operation as well as suitable performance compared to the other portable power sources. It appears that all these pre-requisites are matched by the present device/process. To further ameliorate this process, it is envisaged that an increase of electric efficiency may be achieved by improving the reversibility of the process (i.e. decreasing the polarization resistance) and reducing the ohmic resistance.

Acknowledgements

The authors are grateful to the Italian Ministry of Education and Research (MIUR) for the financial support through the FISR Project (Fondo integrativo speciale per la Ricerca, "Celle a combustibile ad elettroliti polimerici e ceramici: dimostrazione di sistemi e sviluppo di nuovi materiali" Decreto 16.10.2000 G.U. no. 278 28.11.2000).

The authors acknowledge Dr. Gaetano Maggio for the thermodynamic analysis.

Appendix A. Supplementary data

Supplementary data associated with this article can be found, in the online version, at doi:10.1016/j.apcatb.2008.11.019.

References

[1] C. Sun, U. Stimming, Journal of Power Sources 171 (2007) 247.
[2] P. Tsiakaras, C. Ahanasiou, G. Marnellos, M. Stoukides, J.E. Ten Elshof, H.J.M. Bouwmeester, Applied Catalysis A: General 169 (2) (1998) 249.
[3] S. Tao, J.T.S. Irvine, Nature Materials 2 (2003) 320.
[4] A. Sin, E. Kopnin, Y. Doubitsky, A. Zaopo, A.S. Aricò, L.R. Gullo, D. La Rosa, V. Antonucci, Journal of Power Sources 164 (2007) 300.
[5] A. Sin, E. Kopnin, Y. Dubitsky, A. Zaopo, A.S. Aricò, L.R. Gullo, D. La Rosa, V. Antonucci, Journal of Power Sources 155 (1) (2005) 68.
[6] A. Civera, M. Pavese, G. Saracco, V. Specchia, Catalysis Today 83 (1–4) (2003) 199.
[7] A. Yan, M. Cheng, Y. Dong, W. Yang, V. Maragou, S. Song, P. Tsiakaras, Applied Catalysis B: Environmental 66 (1–2) (2006) 64.
[8] M. Lo Faro, D. La Rosa, G. Monforte, V. Antonucci, A.S. Aricò, P. Antonucci, Journal of Applied Electrochemistry 37 (2007) 203.
[9] A. Sin, E. Kopnin, Y. Doubitsky, A. Zaopo, A.S. Aricò, L.R. Gullo, D. La Rosa, V. Antonucci, Fuel Cells 6 (2006) 137.
[10] A.S. Aricò, P. Bruce, B. Scrosati, J. Tarascon, W. van Schalkwijk, Nature Materials 4 (2005) 366.
[11] T. Hibino, A. Hashimoto, K. Asano, M. Yano, M. Suzuki, M. Sano, Electrochemical and Solid-State Letters 5 (2002) A242.
[12] S. McIntosh, J.M. Vohs, R.J. Gorte, Journal of the Electrochemical Society 150 (2003) A470.
[13] S. Lee, J.M. Vohs, R.J. Gorte, Journal of the Electrochemical Society 151 (2004) A1319.
[14] Z. Xie, W. Zhu, B. Zhu, C. Xia, Electrochimica Acta 51 (2006) 3052.
[15] O.A. Marina, M. Mogensen, Applied Catalysis A: General 189 (1999) 117.
[16] S.P. Jiang, S.P.S. Badwal, Solid State Ionics 123 (1999) 209.
[17] B. De Boer, M. Gonzalez, H.J.M. Bouwmeester, H. Verweij, Solid State Ionics 127 (2) (2000) 269.
[18] W. Sangtongkitcharoen, S. Assabumrungrat, V. Pavarajarn, N. Laosiripojana, P. Praserthdam, Journal of Power Sources 142 (2005) 75.
[19] S. Assabumrungrat, V. Pavarajarn, S. Charojrochkul, N. Laosiripojana, Chemical Engineering Science 59 (2004) 6017.
[20] M. Lo Faro, R. Bonfiglio, D. La Rosa, L.R. Gullo, V. Antonucci, A.S. Aricò, in: M. Mogensen (Ed.), Proceedings of the Sixth European Solid Oxide Fuel Cell Forum, European Fuel Cell Forum, Lucerne, Switzerland, (2004), p. 105.
[21] M. Suzuki, H. Sasaki, S. Otoshi, in: F. Grosz, S. Zegers, C. Singhal, O. Yamamoto (Eds.), Proceedings of the Second International Symposium of SOFC's, Athens, (1991), p. 323.
[22] M.J. Saeki, H. Uchida, M. Watanabe, Catalysis Letters 26 (1994) 149.
[23] Z. Zhan, S.A. Barnett, Science 308 (2005) 844.
[24] J. Liu, B.D. Madsen, Z. Ji, S.A. Barnett, Electrochemical and Solid State Letters 5 (6) (2002) A122.
[25] J.W. Johnson, E.H. Oelkers, H.C. Helgeson, Computers & Geosciences 8 (7) (1992) 899.
[26] A. Munoz, J.A. Alonso, M.J. Martinez Lope, C. de la Calle, M.T. Fernandez Diaz, Journal of Solid State Chemistry 179 (2006) 3365.
[27] J.F. Moulder, W.F. Stickle, P.E. Sobol, K.D. Bomben, Handbook of X-ray Photoelectron Spectroscopy, Physical Electronics, Inc., Eden Prairie, MN, USA, 1995, ISBN: 0-9648124-1-X.
[28] N.V. Skorodumova, S.I. Simak, B.I. Lundqvist, I.A. Abrikosov, B. Johansson, Physical Review Letters 89 (2002) 166601–166611.
[29] S. McIntosh, H. He, S.-I. Lee, O. Costa-Nunes, V.V. Krishnan, J.M. Vohs, R.J. Gorte, Journal of Electrochemical Society 151 (2004) A604.
[30] C.Y. Sheng, A.M. Dean, Journal of Physical Chemistry A 108 (2004) 3772.
[31] T. Kim, G. Liu, M. Boaro, S.-I. Lee, J.M. Vohs, R.J. Gorte, O.H. Al-Madhi, B.O. Dabbousi, Journal of Power Sources 155 (2006) 231.
[32] J.A. Kilner, Faraday Discussions 134 (2007) 9.
[33] V. Modafferi, G. Panzera, V. Baglio, F. Frusteri, P.L. Antonucci, Applied Catalysis A: General 334 (2008) 1.
[34] R. Burch, M.J. Hayes, Journal of Molecular Catalysis A: Chemical 100 (1995) 13.
[35] A. Bieberle-Hütter, D. Beckel, A. Infortuna, U.P. Muecke, J.L.M. Rupp, L.J. Gauckler, S. Rey-Mermet, P. Muralt, N.R. Bieri, N. Hotz, M.J. Stutz, D. Poulikakos, P. Heeb, P. Müller, A. Bernard, R. Gmür, T. Hocker, Journal of Power Sources 177 (2008) 123.